Statistics of low energy excitations for the directed polymer in a $1+d$ random medium ($d=1,2,3$)

Cécile Monthus and Thomas Garel
Service de Physique Théorique, CEA/DSM/SPhT Unité de recherche associée au CNRS, 91191 Gif-sur-Yvette cedex, France
(Received 9 February 2006; published 8 May 2006)

We consider a directed polymer of length L in a random medium of space dimension $d=1,2,3$. The statistics of low energy excitations as a function of their size l is numerically evaluated. These excitations can be divided into bulk and boundary excitations, with respective densities $\rho_L^{bulk}(E=0,l)$ and $\rho_L^{boundary}(E=0,l)$. We find that both densities follow the scaling behavior $\rho_L^{bulk,boundary}(E=0,l)=L^{-1-\theta_d}R^{bulk,boundary}(x=l/L)$, where θ_d is the exponent governing the energy fluctuations at zero temperature (with the well-known exact value $\theta_1=1/3$ in one dimension). In the limit $x=l/L\to 0$, both scaling functions $R^{bulk}(x)$ and $R^{boundary}(x)$ behave as $R^{bulk,boundary}(x)\sim x^{-1-\theta_d}$, leading to the droplet power law $\rho_L^{bulk,boundary}(E=0,l)\sim l^{-1-\theta_d}$ in the regime $1\ll l\ll L$. Beyond their common singularity near $x\to 0$, the two scaling functions $R^{bulk,boundary}(x)$ are very different: whereas $R^{bulk}(x)$ decays monotonically for $0<x<1$, the function $R^{boundary}(x)$ first decays for $0<x<x_{min}$, then grows for $x_{min}<x<1$, and finally presents a power law singularity $R^{boundary}(x)\sim(1-x)^{-\sigma_d}$ near $x\to 1$. The density of excitations of length $l=L$ accordingly decays as $\rho_L^{boundary}(E=0,l=L)\sim L^{-\lambda_d}$ where $\lambda_d=1+\theta_d-\sigma_d$. We obtain $\lambda_1\simeq 0.67$, $\lambda_2\simeq 0.53$, and $\lambda_3\simeq 0.39$, suggesting the possible relation $\lambda_d=2\theta_d$.

DOI: 10.1103/PhysRevE.73.056106 PACS number(s): 65.60.+a, 05.40.−a

I. INTRODUCTION

The model of a directed polymer in a random medium has attracted a lot of attention in the last twenty years for two main reasons. On the one hand, it is directly related to nonequilibrium growth models [1]; on the other hand, it plays the role of a "baby spin glass" model in the field of disordered systems [1–5]. This model presents a low temperature disorder dominated phase, where the order parameter is an "overlap" [2,4,6,7]. This low temperature phase displays an extreme sensitivity with respect to temperature or disorder changes [5,8–14], and aging properties for the dynamics [15]. In finite dimensions, a scaling droplet theory was proposed [5,16], in direct correspondence with the droplet theory of spin glasses [17], whereas in the mean-field version of the model on the Cayley, a freezing transition very similar to the one occurring in the random energy model was found [2]. The phase diagram as a function of space dimension d is the following [1]: for $d>2$, there exists a phase transition between the low temperature disorder-dominated phase and a free phase at high temperature [18,19]. This phase transition has been studied numerically in $d=3$ [20,21], exactly on a Cayley tree [2] and on hierarchical lattice [22]. On the contrary, in dimension $d\leqslant 2$, there is no free phase, i.e., any initial disorder drives the polymer into the strong disorder phase. In this paper, we will be interested in the low energy excitations above the ground state in dimensions $d=1,2,3$.

In disordered systems, there can be states that have an energy very close to the ground state energy but which are very different from the ground state in configuration space. For spin glasses, the debate between the droplet and replica theories concerns the probabilities and the properties of these states. In the droplet theory [17], the low temperature physics is described in terms of rare regions with nearly degenerate excitations which appear with a probability that decays with a power law of their size. In the replica theory [23], the replica symmetry breaking is interpreted as the presence of many pure states in the thermodynamic limit, i.e., the nearly degenerate ground states appear with a finite probability for arbitrary large size. More generally, the statistical properties of the nearly degenerate excitations (their numbers, their sizes, their geometric properties, the barriers separating them, etc. …) are interesting in any disordered system, since they govern all properties at very low temperature. In particular, a linear behavior in temperature of the specific heat $C(T)=bT+O(T^2)$ seems rather generic for a large class of disordered models, including (i) spin glasses where this behavior is measured experimentally [24] and numerically [25], (ii) disordered elastic systems [26] (iii) one-dimensional (1D) spin models where this behavior can be exactly computed via the Dyson-Schmidt method [27]. For the last case, the coefficient b of the linear term of the specific heat can be put in direct correspondence with the density $\rho(E=0,l)$ of two-level low energy excitations of size l [28–30] via the simple formula $b=(\pi^2/6)\int dl\rho(E=0,l)$. Other integrals like $\int dll^k\rho(E=0,l)$ with $k=1,2,\ldots$ determine the low temperature behavior of other observables. The explicit computation of the density $\rho(E=0,l)$ of excitations as a function of their size l has been possible only for one-dimensional models, such as the case of one particle in a random potentials [28,29] and the random field Ising chain via strong disorder renormalization [29]. For higher dimensional disordered systems, the statistics of excitations can only be studied numerically. In particular, there has been a lot of efforts to characterize the distribution and the topology of the low energy excitations in of spin glasses [31]. For the directed polymer model in finite dimensions, we are only aware of the work of Tang [32], where the probability of two degenerate nonoverlapping ground states with binary disorder in $1+1$ was found to decay as $L^{-2/3}$. Our aim in this paper is to measure the statistics $\rho_L(E=0,l)$ of low energy excitations of length l, for a directed polymer of length L in a Gaussian random potential, in dimensions $d=1,2,3$. We compare our results with the droplet scaling theory in finite dimensions [5,16]. We also try to make the connection with

the exact results [2] on the Cayley tree ($d=\infty$).

The paper is organized as follows. In Sec. II, we briefly recall known results on the directed polymer in a random medium, concerning exact results in $d=1$ and $d=\infty$ (Cayley tree), as well as the spin glass inspired droplet scaling theory. After presenting the parameters of our numerical study in Sec. III, we briefly present our results on ground state energies in Sec. IV, before focusing on low energy excitations. The statistics of boundary and bulk excitations are respectively studied in Sec. V and VI. We finally summarize and discuss our results in Sec. VII.

II. SUMMARY OF PREVIOUS WORK ON DIRECTED POLYMERS AT LOW TEMPERATURE

A. Ground state properties

The probability distribution of the ground state energy E_0 of a directed polymer of length L in dimension $1+d$ is expected to follow a scaling form

$$P_d(E_0,L) \sim \frac{1}{L^{\theta_d}} \mathcal{P}_d\left(\mathcal{E} = \frac{E_0 - L e_0}{L^{\theta_d}} \right), \tag{1}$$

where e_0 represent the ground state energy density per monomer. The exponent θ_d then governs both the fluctuation and the correction to extensivity of the mean value (note that this is not always the case in disordered systems, see e.g. [33]). This result has been proven in $d=1$ with the exact value of the exponent [34–37]

$$\theta_1 = 1/3. \tag{2}$$

For the mean-field version on the Cayley tree ($d=\infty$) one has formally $\theta_\infty=0$ [2]: the width is of order $O(1)$, whereas the correction to the extensive term Le_0 in the averaged value $\overline{E_0(L)}$ is of order $O(\ln L)$ [2]. In finite dimensions $d=2,3,4,5,\ldots$, the exponent θ_d has been numerically measured [38–42]. The values of the Kardar-Parisi-Zhang exponent χ_d measured in [42] for dimensions $d=2,3$ translate into the following values for the directed polymer exponent θ_d

$$\theta_2 = 0.244, \tag{3}$$

$$\theta_3 = 0.186, \tag{4}$$

through the correspondence $\theta_d=\chi_d/(2-\chi_d)$. Note that the existence of a finite upper critical dimension has remained a very controversial issue between the numerical studies [39–42] and various theoretical approaches [43–45]. Beyond the exponent θ, the scaling function $\mathcal{P}_d$ itself is also of interest: it is exactly known in $d=1$ [36,37] (as well as in other geometries [46]), and has been measured numerically in $d=1,2,3$ [38]. On the other hand for the Cayley tree, the scaling distribution was found to depend on the disorder distribution [47]. Another important property of the ground state in finite dimensions d is the probability distribution of its end-point position $\vec{R}_0$ that follows the scaling form

$$Q_d(R_0,L) \sim \frac{1}{(L^{\zeta_d})^d} \mathcal{Q}_d\left(\vec{r}_0 = \frac{\vec{R}_0}{L^{\zeta_d}} \right), \tag{5}$$

where the exponent ζ_d is directly related to the previous exponent θ_d via the simple relation [48]

$$\zeta_d = \frac{1+\theta_d}{2}. \tag{6}$$

This corresponds to a superdiffusive behavior $\zeta > 1/2$ as soon as $\theta > 0$, and in particular in one dimension $\zeta_1 = 2/3$. The probability distribution $Q_d(R_0,L)$ has been studied for the case $d=1$ in [49].

B. Exact identities from the statistical tilt symmetry

In their continuum version, directed polymers in random media belong to a special class of disordered models for which exact remarkable identities for thermal fluctuations can be derived [50]. The Hamiltonian of these models have a deterministic part which consists in quadratic interactions and a random part whose statistics is translation invariant. For the directed polymer in dimension $1+1$, this so-called statistical tilt symmetry leads in particular to the following identity for the fluctuation of the end point r_L [4,5,16]

$$\overline{\langle r_L^2 \rangle - \langle r_L \rangle^2} = TL. \tag{7}$$

Other identities giving relations between higher cumulants can be similarly derived [5,16,50].

The identity (7) is rather surprising at first sight, since the fluctuations of the end point are found to be independent of the disorder and to be exactly the same as in the absence of disorder. The exact result (7) is particularly interesting at very low temperature, since it predicts a linear behavior in T of the second cumulant, and thus puts constraints on the statistics of nearly degenerate excitations. In simpler 1D models of one particle in random potentials one can explicitly relate [28,29] the linear behavior of the position fluctuations to the rare configurations with two nearly degenerate minima $\Delta E \sim T$. For directed polymer in random media, any theory of low energy excitations has to reproduce the result (7), and we will now describe its interpretation within the droplet theory [5,16].

C. Droplet theory for low energy excitations in finite dimensions

The droplet theory for directed polymers [5,16], is very similar to the droplet theory of spin glasses [17]. It is a scaling theory that can be summarized as follows. The exponent θ involved in the fluctuations of the ground state energy E_0 over the samples [see Eq. (1)] also governs the fluctuations of the energy within one sample as the end point varies. As a consequence, if one assumes a scaling distribution analogous to (1), the probability to find a nearly degenerate ground state $\Delta E \sim T$ of order L behaves as T/L^θ, so it is rare, but it corresponds to a very large fluctuation of the end point of order $\Delta r \sim L^\zeta$ with the spatial exponent ζ [see Eq. (5)]. The contribution of these rare nearly degenerate paths to the disorder averaged fluctuations (7) is thus of order (T/L^θ)

$\times (L^{\zeta})^2 = TL^{2\zeta-\theta} = TL$ using the scaling relation (6).

This naive "zero-order" argument has to be refined if one is interested into the density $\rho_L(E=0,l)$ of excitations that involve an arbitrary length l for a polymer of length L. For $1 \ll l \leqslant L$, the droplet theory assumes that the same scalings apply: the probability of an excitation of length l is of order T/l^{θ} and leads to a fluctuation of the end point of order $\Delta r \sim l^{\zeta}$. However now, the crucial notion of "independent excitations" [5] has to be introduced to obtain a consistent picture. Both for spin glasses [17] and for directed polymers [5], the idea is that in a given sample, droplets with neighboring sizes tend to have a big overlap. More precisely for the polymer, two excitations of lengths l_1 and length l_2 with $l_1 \sim l_2$ will typically merge and then follow the same path to join the ground state, as shown by the tree structure of optimal paths to all end points [1]. As a consequence in [5], droplets are considered to be independent only if there is a factor of order 2 between their sizes, and this gives a factor $d \ln l = dl/l$ in all integrations over droplets

$$dl \rho^{indep}(E=0,l) \sim \frac{dl}{l^{\theta+1}}. \tag{8}$$

A more intuitive view of the dl/l factor is to remark that independent excitations stem from a branching process along the ground state path, and that the infinitesimal number of branches between l and $l+dl$ is precisely dl/l.

In summary, the droplet theory predicts a power law distribution of independent excitations, with exponent $(1+\theta)$. Note that the absence of any characteristic scale in l means that there exists some infinite correlation length in the system in the whole low temperature phase. This is in contrast with simpler models like the random field Ising chain [29] or in the spin glass chain in external field [30], where the density of excitations was found to decay exponentially in l, the correlation length being the Imry-Ma length.

D. Exact results for low energy excitations on the Cayley tree

Many exact results for directed polymers on the Cayley tree have been derived by Derrida and Spohn [2]. The point of view of excitations, the most important result concerns the distribution of the overlap in the thermodynamic limit, which is simply the sum of two δ peaks at $q=0$ and $q=1$ in the whole low temperature phase [2]

$$\pi(q) = (1-Y)\delta(q) + Y\delta(q-1), \tag{9}$$

and the distribution of Y over the samples is the same as in the Random Energy Model [51]. In particular, the disorder average of Eq. (9) is [2]

$$\overline{\pi(q)} = \frac{T}{T_c}\delta(q) + \left(1 - \frac{T}{T_c}\right)\delta(q-1), \tag{10}$$

i.e., the overlap is zero with probability T/T_c, and one otherwise. This means that for a polymer of length L, the important excitations are those of length $l \sim L$, and that these excitations keep a finite weight in the limit $L \to \infty$. To understand the origin of this surprising result, Fisher and Huse [5] have computed that the probability to find an excitation of length l which branches off at a distance $s = L - l \ll L$ from the root behaves as $s^{-3/2}$, i.e., using the length notation $l = L - s$

$$\rho_L(E=0,l) \sim \frac{1}{(L-l)^{3/2}}. \tag{11}$$

Finally, Tang has studied numerically the overlap distribution $\overline{P_L(q)}$ for a polymer of finite size L [32] to characterize how the two δ peaks develop in (10): the data for $0 < q < 1$ follow the scaling behavior [see Figs. (4a) and (4b) of [32]]

$$\overline{\pi_L(q)} \sim L^{-1/2}\hat{\pi}(q), \tag{12}$$

where the scaling function $\hat{\pi}(q)$ present the same singularity with exponent $3/2$ near $q \to 0$ and $q \to 1$

$$\hat{\pi}(q) \underset{q\to 0}{\propto} \frac{1}{q^{3/2}}, \tag{13}$$

$$\hat{\pi}(q) \underset{q\to 1}{\propto} \frac{1}{(1-q)^{3/2}}, \tag{14}$$

so that, in the limit $L \to \infty$, $\overline{\pi_{\infty}(q)}$ only contains two δ peaks at $q=0$ and $q=1$ [see Eq. (10)].

III. MODEL AND NUMERICAL DETAILS

In this paper, we present numerical results for the random-bond version of the directed polymer model on a $1+d$ hypercubic lattice. The partition function satisfies the following recursion:

$$Z_{L+1}(\vec{r}) = \sum_{j=1}^{2d} e^{-\beta \epsilon_L(\vec{r}+\vec{e}_j,\vec{r})} Z_L(\vec{r}+\vec{e}_j). \tag{15}$$

The bond energies $\epsilon_L(\vec{r}+\vec{e}_j,\vec{r})$ are random independent variables, drawn with the Gaussian distribution

$$\rho(\epsilon) = \frac{1}{\sqrt{2\pi}} e^{-\epsilon^2/2}. \tag{16}$$

For each dimension d, we now give the typical lengths L we have studied, with the corresponding number n_s of disordered samples:

(i) For $d=1$, $L=50,100,200,300,400,600$, with respective $n_s/10^6 = 160,40,10,4.7,2.5,4.5$.

(ii) For $d=2$, $L=20,40,60,80,100$, with respective $n_s/10^6 = 30,4.4,5.8,2.2,1$.

(iii) For $d=3$, $L=12,18,24,30,36,42$, with respective $n_s/10^6 = 12.5,2.8,0.9,1.6,0.76,0.4$.

We first briefly describe our results on the ground state energy statistics, before we turn to the measure of the density of low energy excitations on which we focus our attention in this paper.

IV. DISTRIBUTION OF THE GROUND STATE ENERGY

A. Scaling distribution

For the sizes L we have considered, the distribution of the ground state energy E_0 follows the scaling form

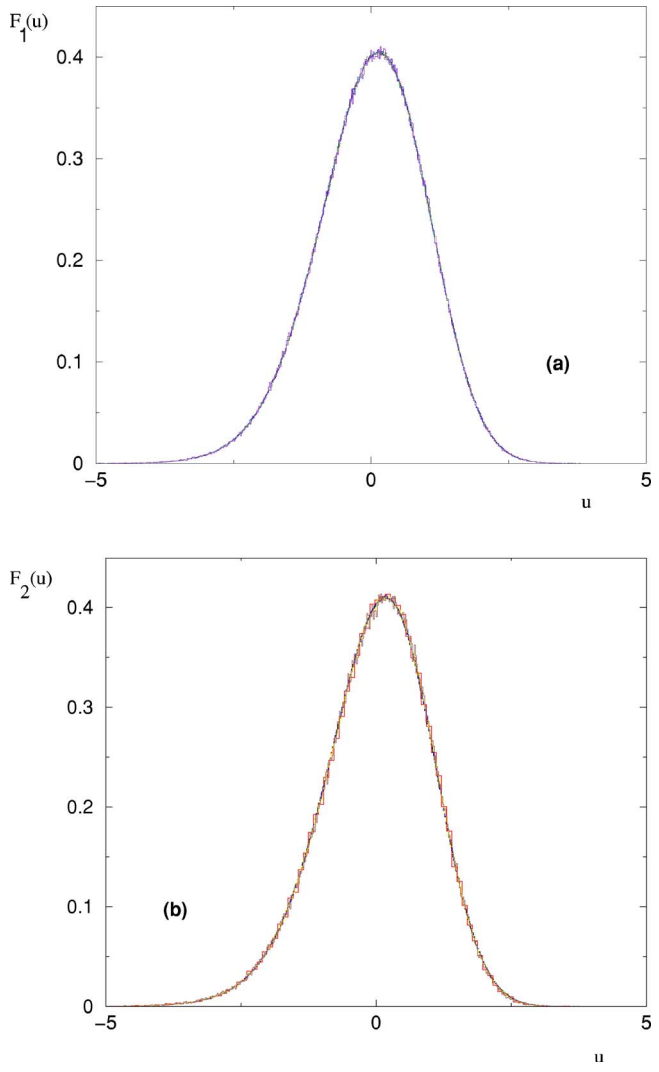

FIG. 1. (Color online) (a) Rescaled distribution $F_1(u)$ of the $d=1$ ground state energy [see Eq. (17)], for $L=50,100,200,300,400,600$. (b) Rescaled distribution $F_2(u)$ of the $d=2$ ground state energy [see Eq. (17)], for $L=10,20,40,80,120$.

$$P_d(E_0,L) \simeq \frac{1}{\Delta E_0(L)} F_d\left(x = \frac{E_0 - E_0^{av}(L)}{\Delta E_0(L)}\right) \tag{17}$$

as shown on Figs. 1(a), 1(b), and 2(a) for $d=1,2,3$ respectively. We have checked that the function $F_1(u)$ of Fig. 1(a) agrees with the numerical tabulation of the exact result given on the web site [52]. The three functions F_1, F_2, F_3 are shown together for comparison on Fig. 2(b).

B. Behavior of the width $\Delta E_0(L)$ and average $E_0^{av}(L)$

The exponent θ_d of Eq. (1) is expected to govern both the width $\Delta E_0(L)$ and the correction to extensivity of the average

$$\Delta E_0(L) \sim L^{\theta_d}, \tag{18}$$

$$\frac{E_0^{av}(L)}{L} \sim e_0(d) + L^{\theta_d - 1} e_1(d) + \cdots. \tag{19}$$

Our measures of the exponent θ_d from the width $\Delta E_0(L)$ yield

$$\theta_1 \sim 0.33, \tag{20}$$

$$\theta_2 \sim 0.24, \tag{21}$$

$$\theta_3 \sim 0.18, \tag{22}$$

are in agreement with the exact value $\theta_1 = 1/3$ and with the previous numerical measures quoted in Eq. (4) for $d=2,3$.

The fits of the average yields

$$d=1: \quad \frac{E_0^{av}(L)}{L} \sim -0.95 + 0.84 L^{\theta_1 - 1} - 1.19 L^{-1}, \tag{23}$$

$$d=2: \quad \frac{E_0^{av}(L)}{L} \sim -1.53 + 1.48 L^{\theta_2 - 1} - 0.94 L^{-1}, \tag{24}$$

$$d=3: \quad \frac{E_0^{av}(L)}{L} \sim -1.81 + 2.05 L^{\theta_3 - 1} - 1.43 L^{-1}. \tag{25}$$

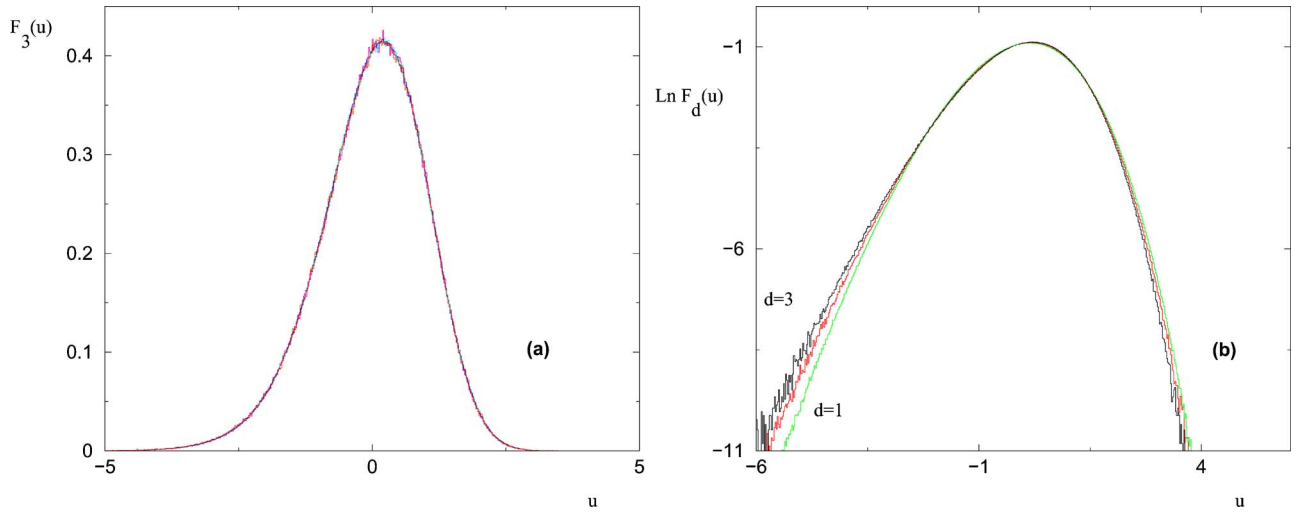

FIG. 2. (Color online) (a) Rescaled distribution $F_3(u)$ of the $d=3$ ground state energy [see Eq. (17)], for $L=6,12,18,24,36$. (b) Comparison of $\ln F_d(u)$ for $d=1,2,3$ [see Eq. (17)].

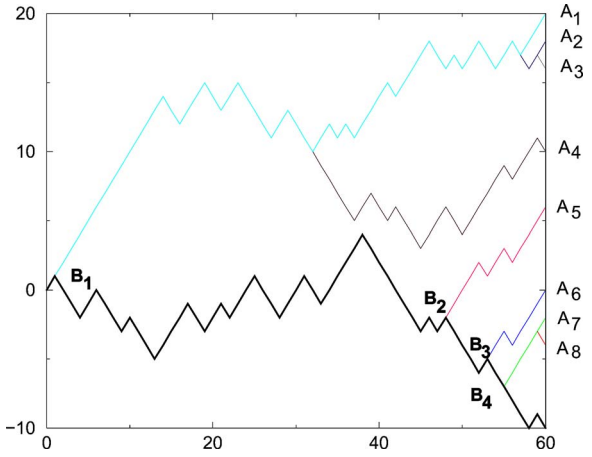

FIG. 3. (Color online) Notion of independent boundary excitations (in $d=1$): for each sample, we generate the ground state (bold line) of energy E_0, and consider all end points A_i where the energy $E(A_i)$ of the best path ending at A_i satisfies $E(A_i)-E_0<T$ (light lines). These best paths tend to cluster into families. In our counting procedure of independent excitations, two excitations are independent if they have no bond in common. For instance on the figure, end points A_1, A_2, A_3, and A_4 count for a single excitation associated to the branch point B_1. Similarly A_7 and A_8 count for a single excitation associated to the branch point B_4.

V. STATISTICS OF BOUNDARY EXCITATIONS

A. Measure of independent excitations

In this section, we are interested into the density $\rho_L^{boundary}(E=0,l)$ of boundary excitations defined as

$$\rho_L^{boundary}(E=0,l)=\lim_{T\to 0}\left[\frac{1}{T}\overline{\mathcal{N}_L^{boundary}(E<T,l)}\right], \quad (26)$$

where $\overline{\mathcal{N}_L^{boundary}(E<T,l)}$ is the disorder averaged number of independent boundary excitations of energy $0<E<T\to 0$ and of length l existing for a directed polymer of length L. This number $\mathcal{N}_L^{indep}(E<T,l)$ is measured as follows. For each sample, we consider all end points $\vec{r}$ different from the ground state $\vec{r}_0$: if the energy $E_{min}(\vec{r})$ of the best path ending at $\vec{r}$ satisfies $E_{min}(\vec{r})-E_0<T$, we construct the best path ending at $\vec{r}$ to measure its length l, i.e., the length over which it is different from the ground state. However, as explained already above when summarizing the droplet theory (8), one is interested into the number of independent excitations. So here we have used the following criterion: two excitations are independent if they have no bond in common. In $d=1$, since we use polymers with $(\pm)$ steps, this means that two excitations are independent if they join the ground state at different points (see Fig. 3). In $d=2$ and $d=3$, two excitations are allowed to join the ground state at the same point provided they branch along two different directions.

In (26), the parameter T is simply a cutoff and we have checked the independence of the density $\rho^{boundary}(E=0,l)$ with respect to T for T small enough. For instance in $d=2$ and $d=3$, we have checked that the cutoffs $T=0.1$ and $T=0.05$ yield the same density $\rho^{boundary}(E=0,l)$.

B. Boundary excitations for $d=1$

On Fig. 4(a), the density $\rho_L^{boundary}(E=0,l)$ is shown in a log-log plot for various sizes L. These curves can be rescaled according to

$$\rho^{boundary}(E=0,l)=\frac{1}{L^{1+\theta_1}}R^{boundary}\left(x=\frac{l}{L}\right) \quad (27)$$

as shown on Fig. 4(b). The master curve $R^{boundary}(x)$ shown on Fig. 5(a) has three important properties

(i) In the region $x\to 0$, the scaling function $R^{boundary}(x)$ follows the power law [see the log-log plot on Fig. 4(b)]

$$R^{boundary}(x)\underset{x\to 0}{\propto}\frac{1}{x^{1+\theta_1}} \quad (28)$$

so that in the regime $1\ll l\ll L$, the statistics of independent excitations

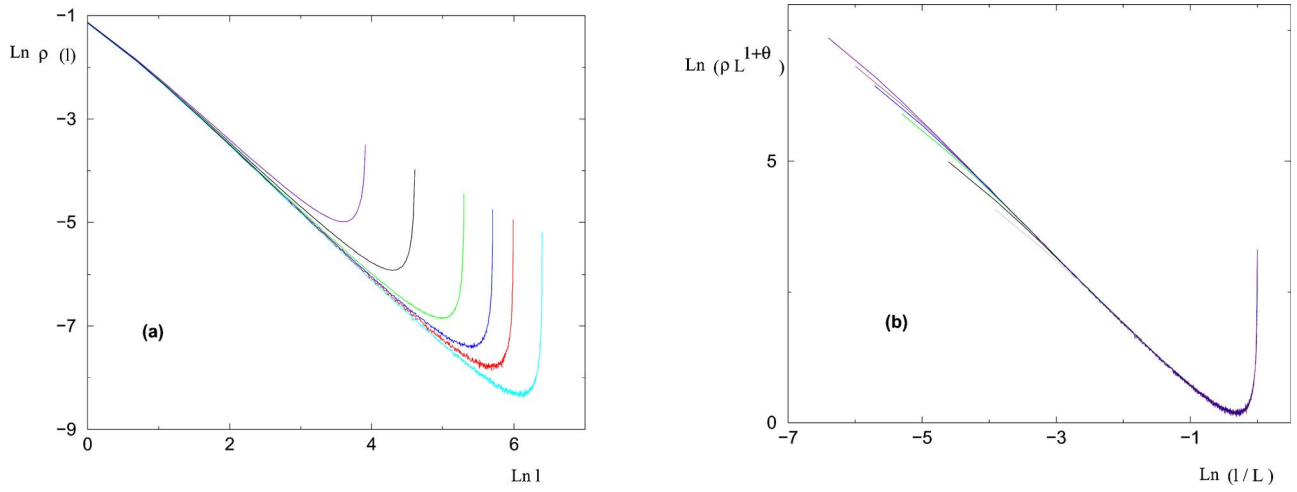

FIG. 4. (Color online) (a) Log-log plot of the density $\rho_L^{boundary}(E=0,l)$ of boundary excitations of length l in $d=1$ for $L=50,100,200,300,400,600$. (b) Same data after the rescaling of Eq. (27) with $\theta_1=1/3$.

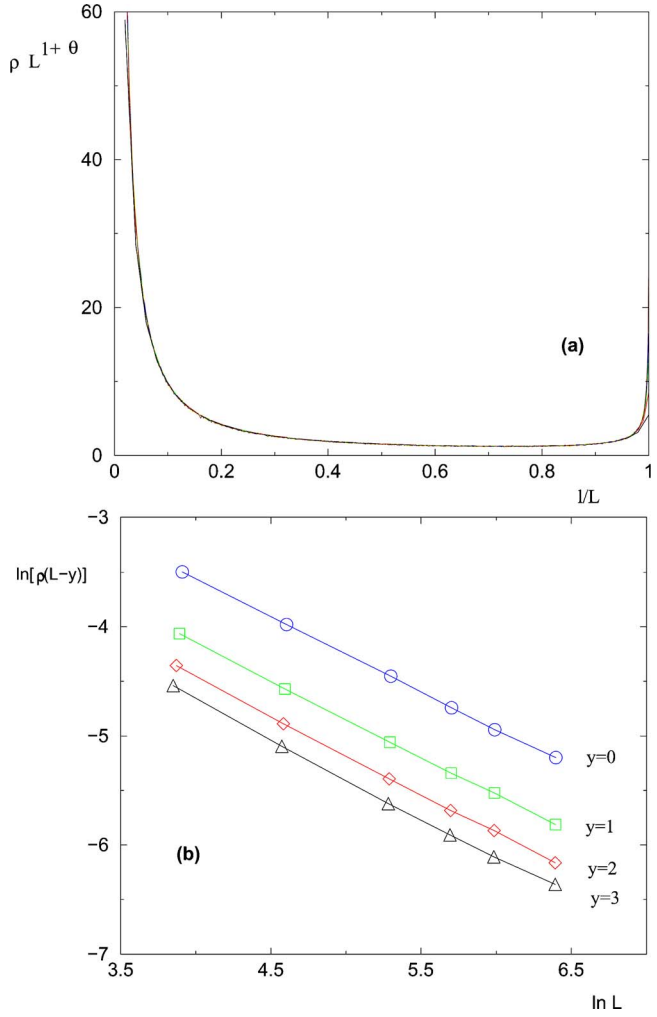

FIG. 5. (Color online) $d=1$: (a) Rescaled distribution $R^{boundary}(x=l/L)$ [see Eq. (27)], that is singular for $x\to 0$ and $x\to 1$. (b) Log-log plot of the density $\rho_L^{boundary}(E=0,l=L-y)$ of very large boundary excitations $l=L-y$ with finite $y=0,1,2,3$.

$$\rho_L^{boundary}(E=0,l)\sim\frac{1}{l^{1+\theta_1}}\quad \text{for } 1\ll l\ll L \tag{29}$$

follows the droplet power law (8).

(ii) The function $R^{boundary}(x)$ is minimum at some finite value $x_{min}(d=1)\sim 0.74$, and then grows for $x_{min}<x<1$.

(iii) In the regime $x=l/L\to 1$, the scaling function $R^{boundary}(x)$ diverges. To describe the regime of these very large excitations, let us first consider the extreme case $l=L$ of an excitation that branches off at the origin. Our result for $l=L$ follow the scaling behavior

$$\rho_L^{boundary}(E=0,l=L)\sim\frac{1}{L^{\lambda_1}}\quad \text{with } \lambda_1\sim 0.67 \tag{30}$$

in agreement with the exponent measured by Tang [32] for the probability of two degenerate ground states in the case of binary disorder. More generally, we find that $\rho_L^{boundary}(E=0,l=L-y)$ with finite y also decays as in (30), see Fig. 5(b). Since the exponent $\lambda_1\sim 0.67$ is different from the exponent $1+\theta_1=4/3$ appearing in the scaling form (27), the singularity of the scaling function $R^{boundary}(x)$ near $x\to 1$ is given by

$$R^{boundary}(x)\underset{x\to 1}{\propto}\frac{1}{(1-x)^{\sigma_1}}\quad \text{with } \sigma_1=1+\theta_1-\lambda_1\sim 0.66. \tag{31}$$

C. Boundary excitations for $d=2$

In $d=2$, we find the same properties for the statistics of boundary excitations with the appropriate exponent $\theta_2\sim 0.24$. The density $\rho_L^{boundary}(E=0,l)$ shown in a log-log plot for various sizes L on Fig. 6(a) follow the scaling form

$$\rho^{boundary}(E=0,l)=\frac{1}{L^{1+\theta_2}}R^{boundary}\left(x=\frac{l}{L}\right) \tag{32}$$

as shown on Fig. 6(b). The master curve $R^{boundary}(x)$ shown on Fig. 7(a) has the same three important properties as in the $d=1$ case.

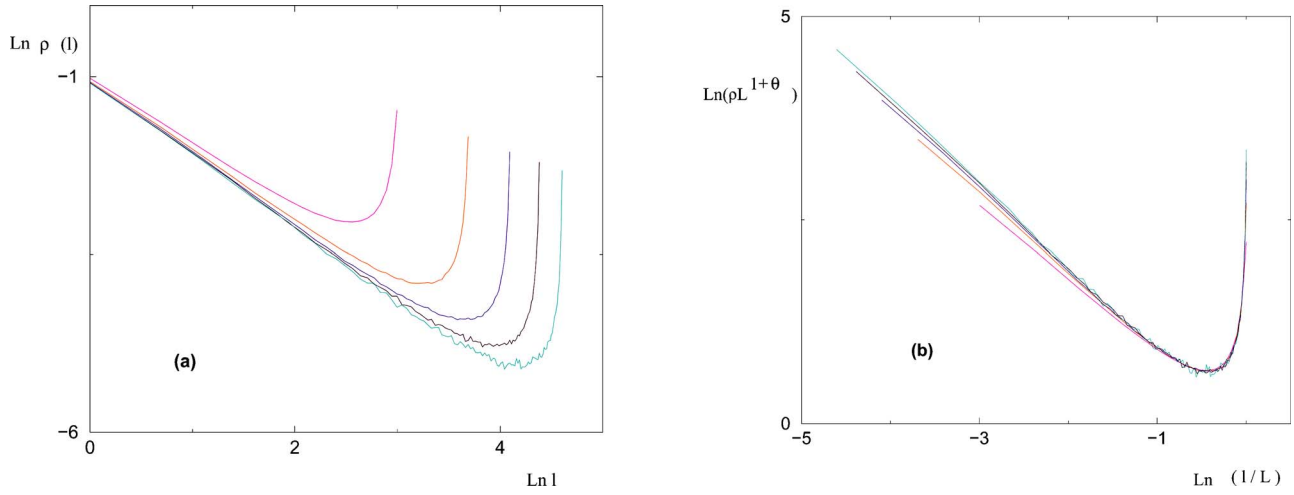

FIG. 6. (Color online) (a) Log-log plot of the density $\rho_L^{boundary}(E=0,l)$ of boundary excitations of length l in $d=2$ for $L=20,40,60,80,100$. (b) Same data after the rescaling of Eq. (32) with $\theta_2\sim 0.24$.

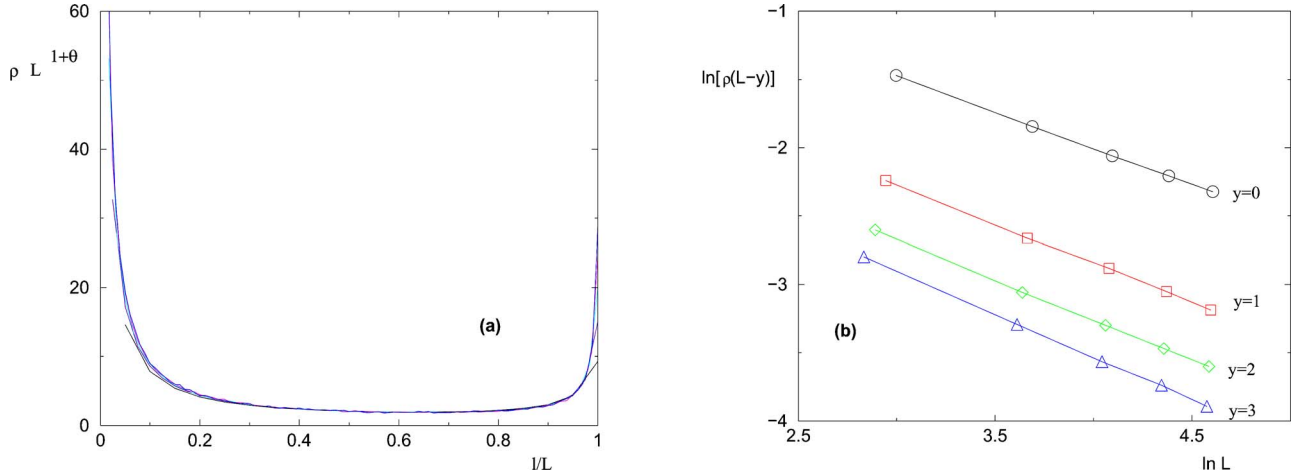

FIG. 7. (Color online) $d=2$: (a) Rescaled distribution $R^{boundary}(x=l/L)$ [see Eq. (32)], that is singular for $x\to 0$ and $x\to 1$. (b) Log-log plot of the density $\rho_L^{boundary}(E=0,l=L-y)$ of very large boundary excitations $l=L-y$ with finite $y=0,1,2,3$.

(i) In the region $x\to 0$, the scaling function follows the power law [see the log-log plot on Fig. 6(b)]

$$R^{boundary}(x) \underset{x\to 0}{\propto} \frac{1}{x^{1+\theta_2}} \tag{33}$$

leading to a statistics of independent excitations

$$\rho_L^{boundary}(E=0,l) \sim \frac{1}{l^{1+\theta_2}} \quad \text{for } 1 \ll l \ll L \tag{34}$$

that follows the droplet power law (8).

(ii) The function $R^{boundary}(x)$ is minimum at some finite value $x_{min}(d=2)\sim 0.64$, and then grows for $x_{min}<x<1$.

(iii) The density of excitations of length $l\sim L$ that branches off at the origin decays with the power law

$$\rho_L^{boundary}(E=0,l=L) \sim \frac{1}{L^{\lambda_2}} \quad \text{with } \lambda_2 \sim 0.53 \tag{35}$$

as shown on Fig. 7(b). So the singularity of the scaling function $R^{boundary}(x)$ near $x\to 1$ is given by

$$R^{boundary}(x) \underset{x\to 1}{\propto} \frac{1}{(1-x)^{\sigma_2}} \quad \text{with } \sigma_2 = 1+\theta_2-\lambda_2 \sim 0.71. \tag{36}$$

D. Boundary excitations for $d=3$

In $d=3$, we find again the same properties for the statistics of boundary excitations with the appropriate exponent $\theta_3 \sim 0.18$. The density $\rho_L^{boundary}(E=0,l)$ shown in a log-log plot for various sizes L on Fig. 8(a) follow the scaling form

$$\rho^{boundary}(E=0,l) = \frac{1}{L^{1+\theta_3}} R^{boundary}\left(x=\frac{l}{L}\right) \tag{37}$$

as shown on Fig. 8(b). The master curve $R^{boundary}(x)$ shown on Fig. 9(a) has the same three important properties as in the previous cases.

(i) In the region $x\to 0$, the power law [see the log-log plot on Fig. 8(b)]

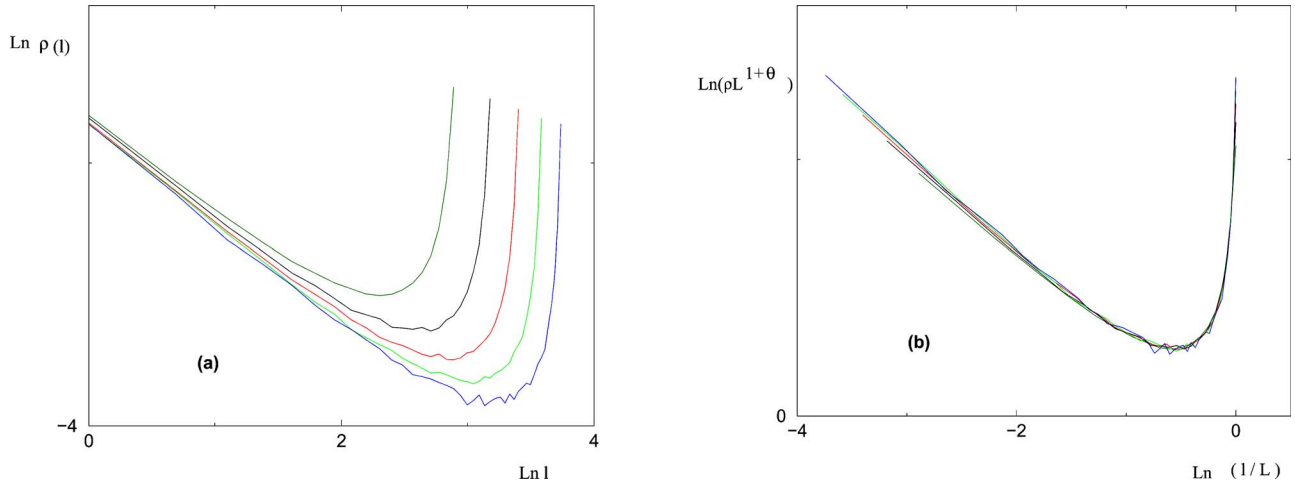

FIG. 8. (Color online) (a) Log-log plot of the density $\rho_L^{boundary}(E=0,l)$ of boundary excitations of length l in $d=3$ for $L=18,24,30,36,42$ (b) Same data after the rescaling of Eq. (37) with $\theta_3\sim 0.18$.

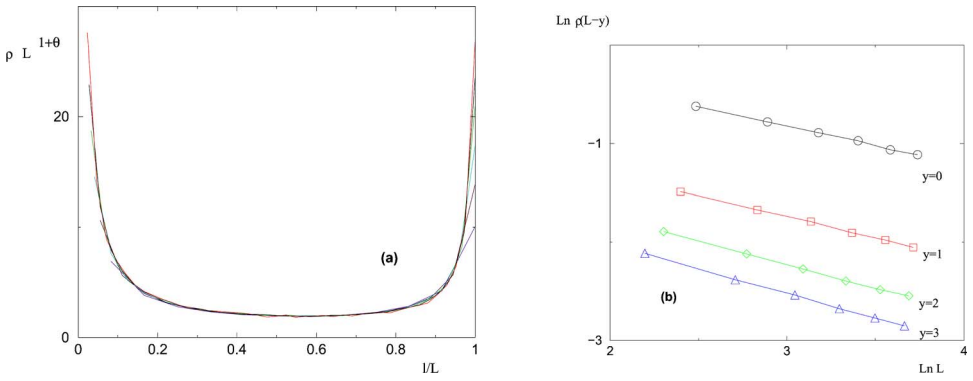

FIG. 9. (Color online) $d=3$: (a) Rescaled distribution $R^{boundary}(x=l/L)$ [see Eq. (37)], that is singular for $x\to 0$ and $x\to 1$. (b) Log-log plot of the density $\rho_L^{boundary}(E=0,l=L-y)$ of very large boundary excitations $l=L-y$ with finite $y=0,1,2,3$.

$$R^{boundary}(x) \underset{x\to 0}{\propto} \frac{1}{x^{1+\theta_3}} \tag{38}$$

leads to a statistics of independent excitations

$$\rho_L^{boundary}(E=0,l) \sim \frac{1}{l^{1+\theta_3}} \quad \text{for } 1 \ll l \ll L \tag{39}$$

that follows the droplet power law (8).

(ii) The function $R^{boundary}(x)$ is minimum at some finite value $x_{min}(d=3)\sim 0.56$, and then grows for $x_{min}<x<1$.

(iii) The density of excitations of length $l\sim L$ that branches off at the origin decays with the power law

$$\rho_L^{boundary}(E=0,l=L) \sim \frac{1}{L^{\lambda_3}} \quad \text{with } \lambda_3 \sim 0.39 \tag{40}$$

as shown on Fig. 9(b). So the singularity of the scaling function $R^{boundary}(x)$ near $x\to 1$ is given by

$$R^{boundary}(x) \underset{x\to 1}{\propto} \frac{1}{(1-x)^{\sigma_3}} \quad \text{with } \sigma_3 = 1+\theta_3-\lambda_3 \sim 0.79. \tag{41}$$

VI. STATISTICS OF BULK EXCITATIONS

A. Measure of independent excitations

We now turn to the density $\rho_L^{bulk}(E=0,l)$ of bulk excitations defined as

$$\rho_L^{bulk}(E=0,l) = \lim_{T\to 0}\left[\frac{l}{TL}\overline{\mathcal{N}_L^{bulk}(E<T,l)}\right], \tag{42}$$

where $\overline{\mathcal{N}_L^{bulk}(E<T,l)}$ is now the disorder averaged number of independent bulk excitations of energy $0<E<T\to 0$ and of length l existing in the bulk for a directed polymer of length L. Here the additional normalization factor (l/L) with respect to the analog definition of boundary excitations (26) ensures a coherent normalization between the two densities $\rho^{boundary}$ and ρ^{bulk}: $\rho^{boundary}(E=0,l)$ represents the probability that the end monomer belongs to an excitation of length l, whereas ρ^{bulk} represents the probability that a bulk monomer belongs to an excitation of length l. The number $\mathcal{N}_L^{indep}(E<T,l)$ is measured as follows. For each sample, we consider all points $\vec{r}_0(t)$ of the ground state with $t=L,L-1,\ldots,2$ as possible end points of bulk excitations. We consider the best paths joining the ground state at $\vec{r}_0(t)$ but arriving from different points than $\vec{r}_0(t-1)$, to see if they have an relative energy with respect to the ground state smaller than the cutoff T. If this is the case, we have found a bulk excitation, and we measure its length l, i.e., the length over which it is different from the ground state. Again, as for boundary excitations, we are interested into independent excitations, and we use the criterion according to which two excitations are independent if they have no bond in common. In $d=1$, since we use polymers with $(\pm)$ steps, this means that two excitations are independent if they join the ground state at different points (see Fig. 10). In $d=2$ and $d=3$, two excitations are allowed to join the ground state at the same point provided they branch along two different directions.

In dimension $d=1,2,3$, we find that the density of bulk excitations follows the scaling form

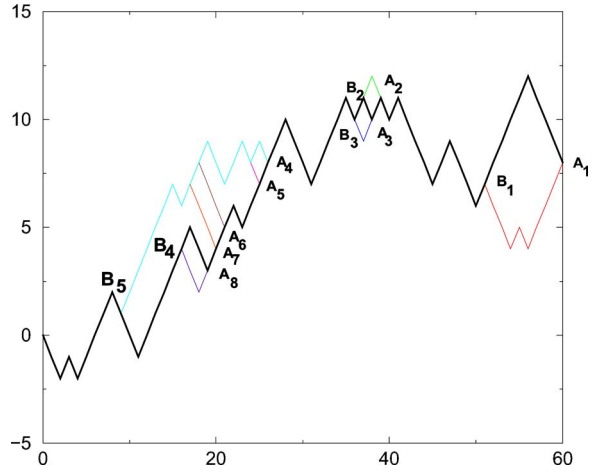

FIG. 10. (Color online) Notion of independent bulk excitations (in $d=1$): for each sample, we generate the ground state (bold line) and consider all points A_i of the ground state, with partial energy $E_0(A_i)$. When the energy $E_1(A_i)$ of the second best path ending at A_i satisfies $E_1(A_i)-E_0(A_i)<T$, we construct these bulk excitations (light lines) that join again the ground state at some branch point B_j. These bulk excitations tend to cluster into families. In our counting procedure of independent excitations, two excitations are independent if they have no bond in common. For instance on the figure, end points A_4, A_5, A_6, and A_7 count for a single excitation associated to the branch point B_5. The other independent excitations are (A_1,B_1), (A_2,B_2), (A_3,B_3), and (A_8,B_4).

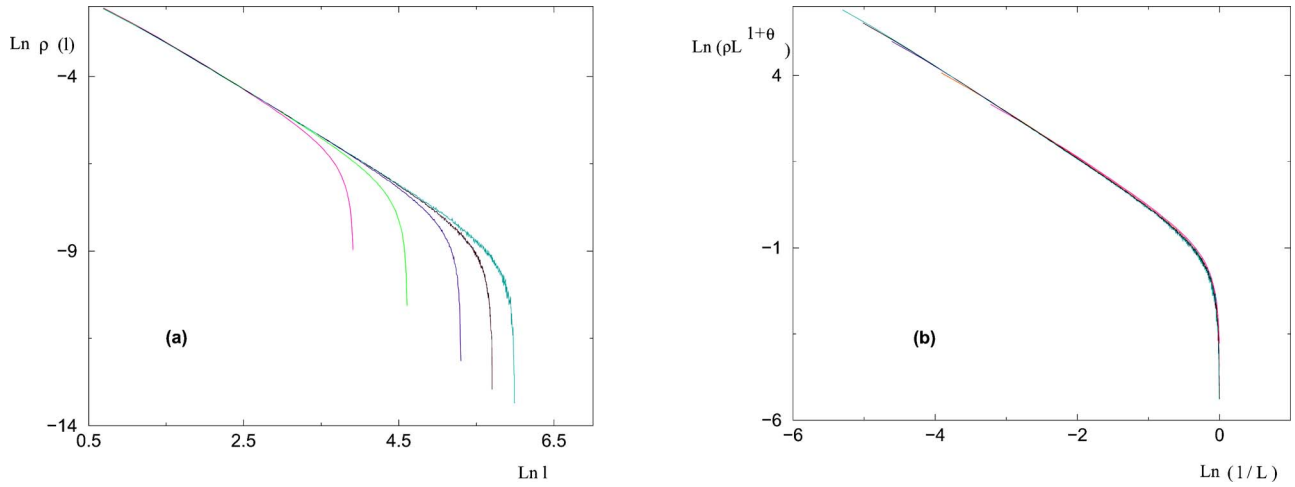

FIG. 11. (Color online) (a) Log-log plot of the density $\rho_L^{bulk}(E=0,l)$ of bulk excitations of length l in $d=1$ for $L=50,100,200,300,400$. (b) Same data after the rescaling of Eq. (43) with exponent $\theta_1=1/3$.

$$\rho^{bulk}(E=0,l)=\frac{1}{L^{1+\theta_d}}R^{bulk}\left(x=\frac{l}{L}\right). \tag{43}$$

See Figs. 11–13 for $d=1,2,3$ respectively. As d increases, the quality of the rescaling gets weaker, because of the smaller sizes L that can be studied via transfer matrix.

In contrast with the scaling function $R^{boundary}(x)$ of boundary excitations, the scaling function $R^{bulk}(x)$ decays monotonically for $0<x<1$. In the region $x\to 0$, the scaling function follows the power law

$$R^{bulk}(x)\underset{x\to 0}{\propto}\frac{1}{x^{1+\theta_d}} \tag{44}$$

so that in the regime $1\ll l\ll L$, the statistics of independent excitations

$$\rho_L^{bulk}(E=0,l)\sim\frac{1}{l^{1+\theta_d}}\quad \text{for } 1\ll l\ll L \tag{45}$$

follows the droplet power law (8).

VII. SUMMARY AND CONCLUSIONS

We have studied the low energy excitations of a directed polymer in a $1+d$ random medium. For dimensions $d=1,2,3$, we find that the densities of bulk and boundary excitations follow the scaling behavior $\rho_L^{bulk,boundary}(E=0,l)=L^{-1-\theta_d}R^{bulk,boundary}(x=l/L)$. In the limit $x=l/L\to 0$, both scaling functions $R^{bulk}(x)$ and $R^{boundary}(x)$ behave as $R^{bulk,boundary}(x)\sim x^{-1-\theta_d}$, leading to the droplet power law $\rho_L^{bulk,boundary}(E=0,l)\sim l^{-1-\theta_d}$ in the regime $1\ll l\ll L$. Beyond their common singularity near $x\to 0$, the two scaling functions $R^{bulk,boundary}(x)$ are very different (this shows the importance of boundary conditions): whereas $R^{bulk}(x)$ decays monotonically for $0<x<1$, the function $R^{boundary}(x)$ first decays for $0<x<x_{min}$, then grows for $x_{min}<x<1$, and finally presents a power law singularity $R^{boundary}(x)\sim(1-x)^{-\sigma_d}$ near $x\to 1$. The density of excitations of length $l\sim L$ decays as $\rho_L^{boundary}(E=0,l=L)\sim L^{-\lambda_d}$ where $\lambda_d=1+\theta_d-\sigma_d$. Our numerical estimates $\lambda_1\simeq 0.67$, $\lambda_2\simeq 0.53$, and $\lambda_3\simeq 0.39$ suggest the relation $\lambda_d=2\theta_d$, although we are not aware of any

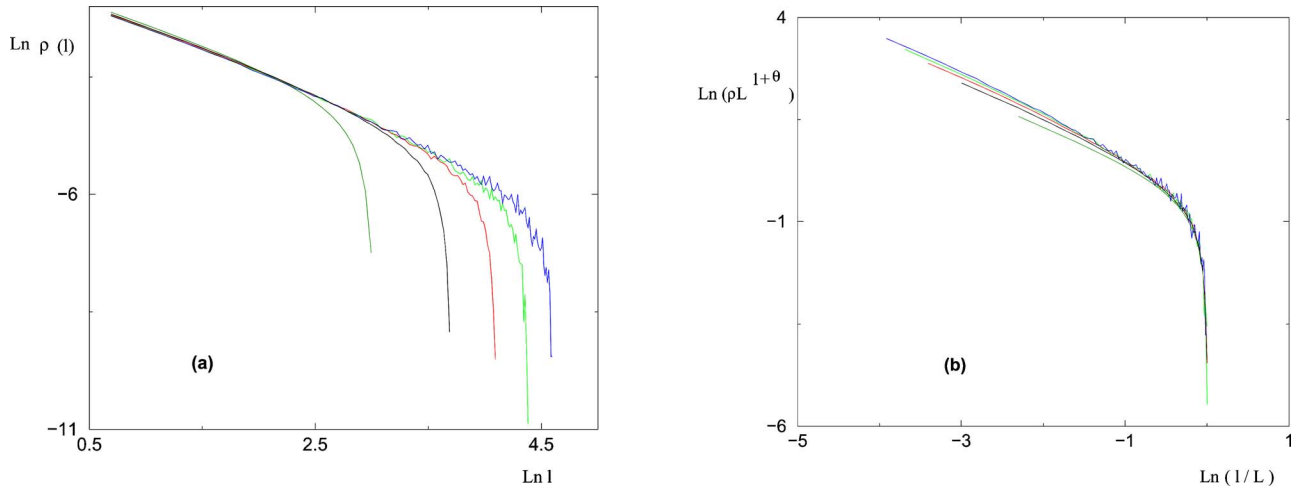

FIG. 12. (Color online) (a) Log-log plot of the density $\rho_L^{bulk}(E=0,l)$ of bulk excitations of length l in $d=2$ for $L=20,40,60,80,100$. (b) Same data after the rescaling of Eq. (43) with exponent $\theta_2=0.24$.

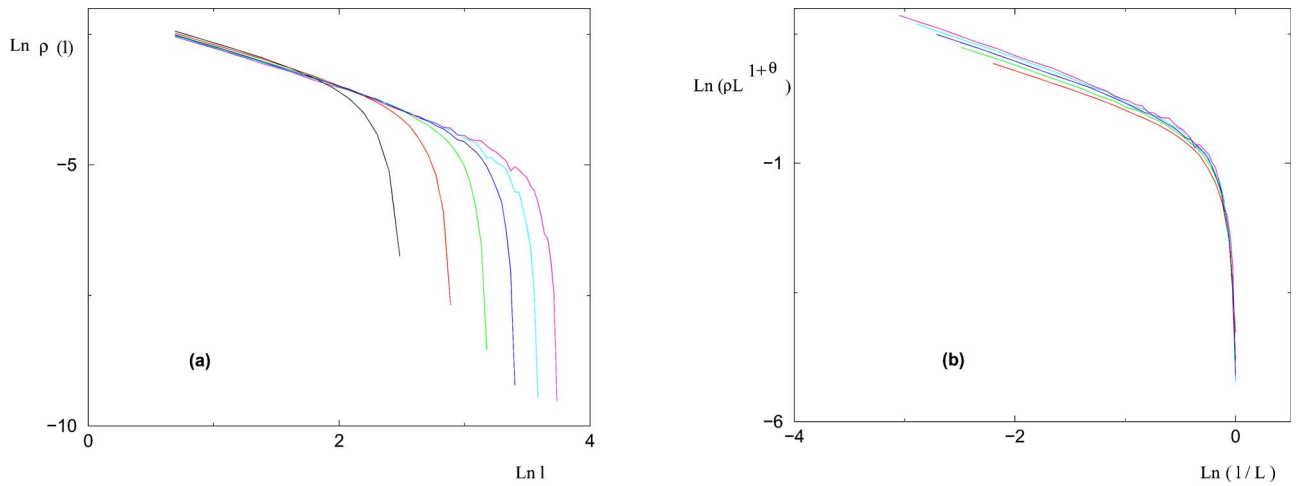

FIG. 13. (Color online) (a) Log-log plot of the density $\rho_L^{bulk}(E=0,l)$ of bulk excitations of length l in $d=3$ for $L=18,24,30,36,42$. (b) Same data after the rescaling of Eq. (43) with exponent $\theta_3=0.18$.

simple argument to justify it. However, if it holds, this would mean that the scaling function $R^{boundary}(x)$ has singularities with exponents $(1+\theta_d)$ and $(1-\theta_d)$ near $x\to 0$ and $x\to 1$ respectively, i.e., these singularities tend to become the same as θ_d decreases, i.e., as the dimension d increases (see Fig. 14). This trend is reminiscent of the result on the Cayley tree discussed in Eqs. (12) and (14) where the singularities have the same exponent on both sides, even if the value (3/2) seems specific to the tree structure and cannot be obtained as the limit $\theta_d=0$ in our results.

Let us now mention how one recovers the identity (7) of the statistical tilt symmetry. A boundary excitation of length l is expected to give rise to a fluctuation of the end point of order $\Delta r\sim l^{\zeta}$ (we temporarily drop the dimension dependence of the exponents), so that at order T, one gets

$$\overline{\langle \Delta r^2\rangle} \sim T\int_1^L dl l^{2\zeta}\rho_L^{boundary}(E=0,l). \tag{46}$$

The contribution of excitations of length l with $x=l/L$ finite reads

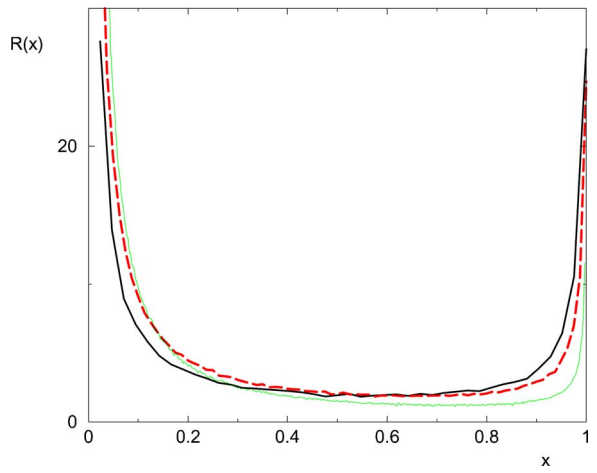

FIG. 14. (Color online) Comparison of the scaling function $R^{boundary}(x)$ for $d=1$ (thin line), $d=2$ (dashed line), and $d=3$ (thick line).

$$[\overline{\langle \Delta r^2\rangle}]_{0<x<1} = TL^{2\zeta-\theta}\int_0^1 dx x^{2\zeta}R^{boundary}(x), \tag{47}$$

whereas the contribution of very large excitations of length $l=L-y$ with finite y reads

$$[\overline{\langle \Delta r^2\rangle}]_{x\sim 1} \sim TL^{2\zeta-\lambda}. \tag{48}$$

Since $\lambda>\theta$, the leading contribution is the first one. Using the scaling relation (6), this contribution is of order $L^{2\zeta-\theta}=L$, as it should to recover (7).

Finally, since the directed polymer model plays the role of a "baby spin glass," and since various numerical studies on spin glasses [31] find both the droplet scaling behavior for small excitations and system-size excitations governed by another "global" exponent, one may wonder whether both types of excitations can be understood within a single scaling function $R(x)$ of the volume fraction $x=v/V$, where the droplet exponent describes the power law in the regime $x\to 0$, whereas the statistics of system-size excitations depends on the global properties of the scaling function $R(x)$. To avoid confusion with the definitions of various θ exponents introduced in the spin-glass literature (θ_l for "local" excitations, θ_g for "global excitations," θ for the exponent of the droplet theory, θ_{DW} for the domain-wall exponent [31], and the exponents λ_l, θ_l of the first excited state in each sample [53]), we recall here that the two exponents θ and λ used in this paper are defined as follows (i) the exponent θ is the exponent of the droplet theory for the directed polymer and governs the statistics of low-energy excitations $\rho_L(E=0,l)\sim 1/l^{1+\theta}$ in the regime $1\ll l\ll L$, (ii) the exponent λ governs the statistics of boundary excitations of length $l=L-O(1)$ with $\rho_L(E=0,L-O(1))\sim 1/L^{\lambda}$, (iii) the statistics of excitations l with $0<x=l/L<1$ follows the scaling form $\rho_L(E=0,l)\sim L^{-1-\theta}R(x=l/L)$, involving the droplet θ exponent.

[1] T. Halpin-Healy and Y.-C. Zhang, Phys. Rep. **254**, 215 (1995).
[2] B. Derrida and H. Spohn, J. Stat. Phys. **51**, 817 (1988).
[3] B. Derrida, Physica A **163**, 71 (1990).
[4] M. Mézard, J. Phys. (France) **51**, 1831 (1990).
[5] D. S. Fisher and D. A. Huse, Phys. Rev. B **43**, 10728 (1991).
[6] P. Carmona and Y. Hu, Probab. Theory Relat. Fields **124**, 431 (2002); P. Carmona and Y. Hu, e-print math.PR/0601670.
[7] F. Comets, T. Shiga and N. Yoshida, Bernoulli **9**, No. 4, 705 (2003).
[8] Y. C. Zhang, Phys. Rev. Lett. **59**, 2125 (1987).
[9] M. V. Feigelman and V. M. Vinokur, Phys. Rev. Lett. **61**, 1139 (1988).
[10] Y. Shapir, Phys. Rev. Lett. **66**, 1473 (1991).
[11] E. T. Seppälä and M. J. Alava, Eur. Phys. J. B **21**, 407 (2001).
[12] M. Sales and H. Yoshino, Phys. Rev. E **65**, 066131 (2002).
[13] R. A. da Silveira and J. P. Bouchaud, Phys. Rev. Lett. **93**, 015901 (2004).
[14] P. Le Doussal, e-print cond-mat/0505679.
[15] H. Yoshino, J. Phys. A **29**, 1421 (1996).
[16] T. Hwa and D. S. Fisher, Phys. Rev. B **49**, 3136 (1994).
[17] D. S. Fisher and D. A. Huse, Phys. Rev. B **38**, 386 (1988).
[18] J. Z. Imbrie and T. Spencer, J. Stat. Phys. **52**, 609 (1988).
[19] J. Cook and B. Derrida, J. Stat. Phys. **57**, 89 (1989).
[20] B. Derrida and O. Golinelli, Phys. Rev. A **41**, 4160 (1990).
[21] J. M. Kim, A. J. Bray, and M. A. Moore, Phys. Rev. A **44**, R4782 (1991).
[22] B. Derrida and R. B. Griffiths, Europhys. Lett. **8**, 111 (1989).
[23] M. Mézard, G. Parisi and M. Virasoro, *Spin Glass Theory and Beyond* (World Scientific, Singapore, 1987).
[24] K. Binder and A. P. Young, Rev. Mod. Phys. **58**, 801 (1986).
[25] J. Houdayer and A. K. Hartmann, Phys. Rev. B **70**, 014418 (2004).
[26] G. Schehr, T. Giamarchi, and P. Le Doussal, Phys. Rev. Lett. **91**, 117002 (2003).
[27] J. M. Luck, *Systèmes désordonnés unidimensionnels* (Aléa, Saclay, 1992); and references therein.
[28] P. Le Doussal and C. Monthus, Physica A **317**, 140 (2003).
[29] C. Monthus and P. Le Doussal, Eur. Phys. J. B **41**, 535 (2004).
[30] C. Monthus and T. Garel, Phys. Rev. B **71**, 094436 (2005).
[31] See for instance: J. Houdayer and O. C. Martin, Europhys. Lett. **49**, 794 (2000); J. Houdayer, F. Krzakala, and O. C. Martin, Eur. Phys. J. B **18**, 467 (2000); F. Krzakala, and O. C. Martin, Phys. Rev. Lett. **85**, 3013 (2000); M. Palassini and A. P. Young, Phys. Rev. Lett. **85**, 3017 (2000); J. Lamarcq, J.-P. Bouchaud, O. C. Martin, and M. Mezard, Europhys. Lett. **58**, 321 (2002); J. Lamarcq, J.-P. Bouchaud, and O. C. Martin, Phys. Rev. B **68**, 012404(R) (2003); M. Palassini, F. Liers, M. Juenger, and A. P. Young, Phys. Rev. B **68**, 064413 (2003); F. Krzakala and G. Parisi, Europhys. Lett. **66**, 729 (2004).
[32] L. H. Tang, J. Stat. Phys. **77**, 581 (1994).
[33] J.-P. Bouchaud, F. Krzakala, and O. C. Martin, Phys. Rev. B **68**, 224404 (2003).
[34] D. A. Huse, C. L. Henley, and D. S. Fisher, Phys. Rev. Lett. **55**, 2924 (1985).
[35] M. Kardar, Nucl. Phys. B **290**, 582 (1987).
[36] K. Johansson, Commun. Math. Phys. **209**, 437 (2000).
[37] M. Prähofer and H. Spohn, Physica A **279**, 342 (2000); M. Prähofer and H. Spohn, Phys. Rev. Lett. **84**, 4882 (2000); M. Prähofer and H. Spohn, J. Stat. Phys. **108**, 1071 (2002); M. Prähofer and H. Spohn, J. Stat. Phys. **115**, 255 (2002).
[38] J. M. Kim, M. A. Moore, and A. J. Bray, Phys. Rev. A **44**, 2345 (1991).
[39] L. H. Tang, B. M. Forrest, and D. E. Wolf, Phys. Rev. A **45**, 7162 (1992).
[40] T. Ala-Nissila, T. Hjelt, J. M. Kosterlitz, and V. Venalainen, J. Stat. Phys. **72**, 207 (1993).
[41] T. Ala-Nissila, Phys. Rev. Lett. **80**, 887 (1998); J. M. Kim, Phys. Rev. Lett. **80**, 888 (1998).
[42] E. Marinari, A. Pagnani, and G. Parisi, J. Phys. A **33**, 8181 (2000); E. Marinari, A. Pagnani, G. Parisi, and Z. Racz, Phys. Rev. E **65**, 026136 (2002).
[43] M. Lassig and H. Kinzelbach, Phys. Rev. Lett. **78**, 903 (1997).
[44] F. Colaiori and M. A. Moore, Phys. Rev. Lett. **86**, 3946 (2001).
[45] P. Le Doussal and K. J. Wiese, Phys. Rev. E **72**, 035101(R) (2005).
[46] E. Brunet and B. Derrida, Phys. Rev. E **61**, 6789 (2000).
[47] D. S. Dean and S. N. Majumdar, Phys. Rev. E **64**, 046121 (2001).
[48] D. A. Huse and C. L. Henley, Phys. Rev. Lett. **54**, 2708 (1985).
[49] T. Halpin-Healy, Phys. Rev. A **44**, R3415 (1991).
[50] U. Schulz, J. Villain, E. Brezin, and H. Orland, J. Stat. Phys. **51**, 1 (1988).
[51] B. Derrida and G. Toulouse, J. Phys. (Paris), Lett. **46**, L223 (1985).
[52] M. Prähoher and H. Spohn on their web site http://www-m5.ma.tum./KPZ/.
[53] M. Picco, F. Ritort, M. Sales, Phys. Rev. B **67**, 184421 (2003).